Decoding functional hematopoietic progenitor cells in the adult human lung

Catharina Conrad
University of California, San Francisco
Melia Magnen
University of California, San Francisco
Jessica Tsui
University of California, San Francisco
Harrison Wismer
University of California, San Francisco
Mohammad Naser
UCSF https://orcid.org/0000-0002-9025-2759
Urmila Venkataramani
University of California, San Francisco
Bushra Samad
University of California, San Francisco https://orcid.org/0000-0002-2893-0897
Simon J Cleary
UCSF https://orcid.org/0000-0001-5573-6363
Longhui Qiu
University of California, San Francisco
Jennifer J Tian
University of California, San Francisco
Marco De Giovanni
University of California, San Francisco
Nicole Mende
Wellcome MRC Cambridge Stem Cell Institute, University of Cambridge, Cambridge, UK
https://orcid.org/0000-0002-5078-2333
Emmanuelle Passegue
Columbia University Irving Medical Center https://orcid.org/0000-0002-3516-297X
Elisa Laurenti
University of Cambridge https://orcid.org/0000-0002-9917-9092
Alexis J Combes
University of California, San Francisco https://orcid.org/0000-0002-9110-6542
Mark R Looney (mark.looney@ucsf.edu)
University of California, San Francisco https://orcid.org/0000-0003-0241-9190

Biological Sciences - Article

Keywords: Stem Cell Biology, Hematopoeitic stem and progenitor cells, Extramedullary Hematopoeisis, Erythropoeisis, Stem Cell Transplantation, Blood and Immune Cell Production

Posted Date: February 16th, 2024

DOI: https://doi.org/10.21203/rs.3.rs-3576483/v2

Additional Declarations: The authors declare no competing interests.

Abstract

The bone marrow is the main site of blood cell production in adults, however, rare pools of hematopoietic stem and progenitor cells with self-renewal and differentiation potential have been found in extramedullary organs. The lung is primarily known for its role in gas exchange but has recently been described as a site of blood production in mice. Here, we show that functional hematopoietic precursors reside in the extravascular spaces of the human lung, at a frequency similar to the bone marrow, and are capable of proliferation and engraftment. The organ-specific gene signature of pulmonary and medullary $CD34^+$ hematopoietic progenitors indicates greater baseline activation of immune, megakaryocyte/platelet and erythroid-related pathways in lung progenitors. Spatial transcriptomics mapped blood progenitors in the lung to a vascular-rich alveolar interstitium niche. These results identify the lung as a pool for uniquely programmed blood stem and progenitor cells with the potential to support hematopoiesis in humans.

Introduction

Hematopoietic stem cells (HSCs) are self-renewing cells residing in the bone marrow (BM) that are ultimately responsible for production of all mature circulating blood cell lineages.[1] Despite the burden of maintaining hematopoiesis, HSCs are a rare cell type in the BM accounting for <0.01% of nucleated cells.[2,3] They occupy and are maintained by a specific BM niche yet are able to exit the BM environment and enter the circulation, although the explanation of this behavior is largely unknown.[4] HSCs are central to the pathogenesis of serious disorders including myelodysplasia, acute and chronic leukemia, aplastic anemia[5] and clonal hematopoiesis[6], and HSC transplantation can be a life-saving therapy. Previously, we discovered extravascular hematopoietic stem and progenitor cells (HSPCs) in the adult mouse lung capable of engraftment in the BM and multi-lineage hematopoiesis.[7] Motivated by this background, in this study we sought to determine if HSPCs occupied the adult human lung—an organ with a vast vasculature that contains a wide-ranging repertoire of stromal and immune cells.

The adult human lung contains functional HSPCs

We had the unique opportunity to receive matched adult human lungs, vertebral bodies (BM), and peripheral blood (PB) freshly recovered from deceased research donors (Table S1). The lungs were extensively perfused at the time of collection, and we selected healthy-appearing lung tissue from the upper lobes for experiments (Figure S1A). After tissue dissociation and the rendering of single-cell suspensions, we characterized live, lineage negative (Lin^-) cells (Figure 1A) using standard surface markers for HSPCs (Table S2).[8-10] Notably, our lineage panel contained markers for mature immune, endothelial, and epithelial cells, allowing for the phenotyping of rare Lin^-CD34^+ cells. We discovered a distinct population of multipotent progenitors (MP; ($CD34^+/CD38^-$) in the lung and BM and very few of these cells in the peripheral blood (PB) (Figure 1B). The lung and BM contained cells with surface staining consistent with HSCs ($CD34^+/CD38^-/CD90^+/CD45A^-$) but these cells were absent in the PB.

Multipotent progenitor (MPP) cells ($CD34^+/CD38^-/CD90^-/CD45A^-$) were observed in all three tissues. CMP ($CD34^+/CD38^+/CD45A^-/Flt\text{-}3^+$), GMP ($CD34^+/CD38^+/CD45A^+/Flt\text{-}3^+$), and MEP ($CD34^+/CD38^+/CD45A^-/Flt\text{-}3^-$) cells were observed in all three tissues but were less common in the lung (Figure 1B). Overall, the BM and PB had nearly identical proportions of hematopoietic progenitors, while Lin^- lung cells were enriched for immunophenotypic HSCs and MPPs (Figure 1C). To rule out residual blood as a source of HSPCs in perfused lungs, we estimated the numbers of progenitors in equivalent volumes of blood and lung tissue, yielding lung HSPC numbers that could not be explained by retention of intravascular blood in lungs (Figure S1B). Further, the distinct proportions of cell subsets in lung and blood indicates a tissue-specific progenitor composition (Figure S1C). Remarkably, the frequency of the immunophenotypic HSC/MPP pool in the lung is similar to the BM (Figure 1D), while the pool of more committed hematopoietic progenitor cells is much smaller in the lung (Figure 1D, Figure S1D). We also tested for the effects of donor age and gender on our results and found that increasing age was associated with fewer numbers of HSPC pools in the BM but not in the lung (Figure S2A-B). Gender was not associated with changes in HSPC frequency in the BM or lung (Figure S2C-D).

Since fibroblasts are generally lineage-negative cells, but some can be CD34-positive[11], we included a marker for fibroblasts (PDGFRα) in our lineage panel to determine if fibroblast contamination could affect our results, but we did not detect any changes in HSPC frequencies between our two lineage panels (Figure S3A-C).

We next tested the functional capacity of lung HSPCs using *in vitro* colony forming assays. We plated Lin^- cells from the lung or BM in MethoCult™ and observed a variety of colonies from both tissues. The Lin^- cells from the lung produced overall fewer colonies, but with a significant increase in the relative proportion of erythroid colonies (BFU-E) (Figure 1E). Following morphologic colony assessment, we used flow cytometry (Figure S4A-B) to confirm cellular colony composition and found that lung colonies were enriched with cells expressing the erythrocyte marker GlyA (Figure S4C). We also plated Lin^- cells in MegaCult™ to test the potential to produce megakaryocytes, a cell population that we previously described as resident cells in the mouse lung.[7] Both BM and lung cells were capable of producing megakaryocyte colonies although the lung produced fewer and small colonies (Figure 1F). The fewer colonies observed from lung cells may relate to overall reduced cell cycling compared to the BM (Figure 1G). The molecular cues that regulate the transition to activity in pulmonary HSPCs are not known and could be different from conditions in classical *in vitro* CFU assays. Together, we conclude that the human lung contains functional HSPCs that exhibit an erythroid bias.

Human lung-derived hematopoietic progenitors have engraftment potential

We next tested whether HSPCs isolated from the lung are capable of engraftment when xenotransplanted into immunodeficient mice.[12] We chose NSG-SGM3 mice (human SCF, GM-CSF, IL-3) to support human myeloid cell engraftment[13] for these experiments in which we adoptively transferred magnetic-enriched

Lin$^-$ cells from the lung or BM into mice after sublethal irradiation[14]. Given that the production of erythroid cells in xenograft models is not reliable due to the lack of cross-reactivity between mouse EPO and the human EPO-receptor, mice received recombinant human erythropoietin injections in the final three weeks of the experiment (Figure 2A) as described previously.[12] Human cells in the BM, lung and PB of recipient mice were assessed after 10 weeks, a time point that is commonly used to measure human HSC activity *in vivo*.[14-16] Engraftment was rigorously defined as the presence of human CD45$^+$ cells, using two different antibody clones, with the threshold for engraftment set to ≥0.01% CD45^{++} cells of all CD45$^+$ cells (mouse and human) with at least 30 cells recorded in the CD45^{++} gate for BM and lung, and ≥ 15 cells for PB[12] given that low levels of engrafted human cells are expected from previous studies.[16] Examples of positive and negative engraftment (sublethal irradiation without adoptive cell transfer) are shown in Figure 2B. Overall, 6/7 mice with BM-derived HSPCs and 5/7 mice with lung-derived HSPCs engrafted in the BM and in the lung tissue (Figure 2C, Figure S5A-B). In the PB, engraftment was observed in 4/7 mice with BM-derived HSPCs and 2/7 mice with lung-derived HSPCs (Figure 2C). Examples of BM- or lung-derived cells in the mouse BM or lung are shown in Figure 2D. We also determined erythroid engraftment using the gating strategy in Figure 2E to detect CD45$^-$, hGlyA$^+$, hCD71$^+$ cells and observed similar erythroid engraftment of BM- or lung-derived HSPCs in the mouse BM, lung, or PB (Figure 2F-G). Similar to BM-derived HSPCs, lung-derived HSPCs were capable of multilineage blood cell production (Figure 2H, Figure S5C-E).

Human lung HSPCs have unique transcriptional programming

The availability of matched lung and medullary HSPCs allowed us to directly compare their transcriptional profiles using single-cell RNA-sequencing (scRNA-seq, Figure S6). We integrated all samples using Harmony[17] and generated a batch-corrected UMAP to identify clusters of transcriptionally similar cells. By using the function 'findConservedMarkers' we identified genes that were consistently expressed across BM and lung-derived cells and annotated clusters based on a reference data set.[18,19] Dimensionality reduction yielded a visual representation consistent with HSC and MPP production of progenies with progressive commitment to more differentiated fates (Figure 3A, Figure S6A-B). To validate our annotation, we generated co-regulated modules of differentially expressed genes using Monocle3.[20] The module highly specific for HSCs contains genes such as *AVP, SPINK2, SELL* and *HOPX* and was strongly expressed in cells from both the BM and lung (Figure 3B, Figure S6C-D). We ordered the cells along a pseudotime trajectory to reconstruct their developmental path for each tissue individually, suggesting a relationship between HSCs and stromal cells in the lung that was absent in cells derived from the BM (Figure 3C). As previously discussed, some pulmonary fibroblasts are CD34$^+$ and these results could point to the ontogeny of a subset of lung stromal cells.

Next, we compared the differential gene expression between medullary and lung cells within the HSC/MPP cluster and plotted the median expression of both cells on a scatter plot (Figure 3D). Using the Wilcoxon rank-sum test in Seurat's 'FindMarkers' we identified 50 genes that were upregulated in lung HSCs and 10 genes that were higher in BM cells (Figure 3D). Among the top upregulated genes in lung

HSCs, several genes (*CEBPB, SOD2, PLCG2, HSPA1A*) were associated with maintaining hematopoietic stem cell quiescence and fitness (Figure 3E).[21-24] We attributed the highest biological relevance to genes that were upregulated in most of the cells, as validated by analyzing the distribution of gene expression values (Figure 3F-H). HSCs from the lung have unique features (Figure 3F) and share characteristics of the hematopoietic lineage (Figure 3G), while as expected, cells from the BM have high expression of classical stem cell genes (Figure 3H).[18]

Next, we performed single-sample Gene Set Enrichment Analysis (ssGSEA) to identify pathways that are differentially regulated between cells from the lung and the BM. The enrichment scores were calculated across all individual cells and tissues for gene set collections from the Molecular Signature Database (H: hallmark, CP: canonical pathways, C5: ontology). In the gene sets analyzed, repeatedly pathways associated with erythropoietin (EPO) signaling, platelet function, and immune responses were found to be upregulated in pulmonary HSCs (Figure 3I). Side-by-side comparison of selected pathways indicates that HSCs from the lung are enriched for megakaryocyte (R-HSA-8936459) and EPO-induced erythroblast (R-HSA-9027277, R-HSA-9006335) differentiation, as indicated by higher normalized enrichment scores (NES) (Figure 3J). Our finding of increased EPO signaling pathways in lung HSCs is consistent with our data in Figure 1E on the erythroid-biasing of lung colonies. Our finding of platelet and megakaryocyte-skewing of lung HSCs is provocative in light of our previous work on platelet production in the lung and tissue-resident immune-like megakaryocytes.[7,25] Additionally, we found inflammatory signaling to be upregulated in pulmonary HSCs (Figure 3K), suggesting that these cells could impart unique immunological functions of their progeny.

A small cluster of cells has recently been suggested as hematopoetic stem cell population in an analysis of the healthy and diseased human lung tissue based on *CD34, SPINK2, STMN* and *PRSS57* expression[26], but the self-renewal and differentiation potential, and the location of these cells is not known. Also, $CD34^+$ cells can be found in endothelial, lymphatic and fibroblast clusters (Figure S7A-B). To identify potential HSCs based on their transcriptomic profile, we used UCell scoring to find Lin^-, $CD34^+$ cells with an HSC signature in a dataset combining 9 human lung scRNA-seq studies (Human Lung Cell Atlas V2, HLCA)[27] (Figure S7C-D). We projected these cells on our UMAP structure of hematopoietic stem and progenitors cells from the lung and BM (Figure 3A) in Figure S7E and mapped 43 cells to the HSC/MPP cluster (Figure S7F) across all integrated datasets in the HLCA (Figure S7G). We conclude that given their rarity and the co-expression of CD34 in multiple lung cell types, lung HSCs are mostly masked and overlooked when using standard unsupervised clustering techniques.

HSPCs in the lung reside in the extravascular tissue

The lung is composed of diverse cell entities, such as epithelial, endothelial, stromal, and immune cell subpopulations that could provide a unique niche for HSPC maintenance and differentiation.[19] To map HSPCs to their lung compartment, we used a spatial transcriptomics approach based on combinatorial single-molecule fluorescent *in situ* hybridization (Figure 4A). We designed a marker panel that

characterizes HSPCs as well as the common cell entities of the lung (Table S3). Following QuPath-based cell segmentation, we filtered for putative HSPCs defined by $CD34^+$ positivity, expression of HSPC-associated transcripts and negativity for marker genes of other lung cell entities (Figure 4B, Figure 8A, B). We visually validated all candidate cells and assigned them to their anatomic location. Over 90% of cells matching the criteria for HSPCs localized to the extravascular lung, with the majority of the cells in the alveolar interstitium or in proximity of bronchi (peribronchial) and vasculature (perivascular) (Figure 4C). To define the neighborhood of HSPCs on the cellular level, we performed unsupervised clustering of the cells generated via segmentation using their transcript expression values (Figure 4D, Figure S8C and Figure S9A-D). Based on this annotation, we used Squidpy for co-occurrence analysis across all samples[28] suggesting that the immediate HSPC niche is mainly formed by endothelial cells, although epithelium and fibroblasts have a steady presence (Figure 4E-F).

Discussion

For many years, HSCs were viewed as unbiased cells that initiated hematopoietic development and specialization. Enabled by new technologies, our understanding of hematopoiesis has been refined to include the possibility that developmental biases may be present even in these most undifferentiated cells, such as with megakaryocyte-biased HSCs.[9] However, the mechanisms responsible for this early biasing or specialization are not clear.[29,30] Here, we propose that the traditional view of HSC residency in the BM should be reconsidered to include extramedullary tissues, such as the lung. Indeed, and remarkably, we found an equal frequency of multipotent progenitors residing in the bone marrow and lung. Due to the low frequency, we used approaches to enrich for the presence of HSPCs in our studies, which were not done in previous studies and likely enabled the profiling of this rare subset of cells amongst the >30 different lung cell types.

It is clear from our studies that the lung HSPCs have unique features compared to their medullary counterparts, but also to HSPCs found at other extramedullary sites (peripheral blood and spleen[31]). Chief amongst these, and perhaps obvious from our understanding of lung biology, is that lung HSPCs, like spleen HSPCs, are less active in terms of cell division and the production of more differentiated and specialized hematopoietic cells than their BM counterparts.[31] These results from *in vitro* experiments would suggest that lung HSPCs function as a reserve pool that could be mobilized in the setting of hematopoietic stress. While physiologically most lung HSPCs might be silenced, a case of pulmonary hematopoesis after sex-mismatched allogeneic stem cell transplantation (SCT) suggests that indeed engraftment into the lung occurs and can lead to active hematopoeisis years after SCT.[32] Further studies are needed to define physiological and pathological stimuli that trigger hematopoiesis in the lung.

Our xenotransplantation experiments indicated that lung HSPCs performed similarly to medullary HSPCs, when given the challenge of engraftment after sublethal irradiation. A wide range of engraftment levels and analysis time points have been used for measuring human HSC activity *in vivo* and there is no standard in the field.[16] Thus, despite low graft expansion in our model (NSG-SGM3 mice, sub-lethal

irradiation, intravenous HSPCs), our data are consistent with previous outcomes and demonstrate self-renewal capacity of pulmonary HSPCs *in vivo*. Additionally, we included donors of any age and sex (Table S1), which might have contributed to larger variations in our results.

Our transcriptomics analysis revealed a distinct molecular program in lung HSPCs that was further distinguishing compared to medullary HSPCs. We found clear megakaryocyte biasing of lung vs. medullary HSPCs indicating that perhaps the lung is a source of these biased progenitors. This is an intriguing finding given (1) the role of the lung in platelet biogenesis and (2) the presence of tissue resident immune-like megakaryocytes (of unclear ontogeny) in the lung.[7] We further found an erythroid bias of lung HSPCs, akin to that reported in peripheral blood and spleen HSPCs.[31] Erythroid bias therefore is a shared feature of steady-state extramedullary HSPCs, perhaps determined by distinct access to environmental oxygen versus the relatively hypoxic environment of the BM.[33]

Our spatial transcriptomic studies were essential in confirming the presence of HSPCs in the lung and defining their precise locations and niche. Given the prevailing dogma that hematopoietic precursors widely circulate[34-36], it was important to rule out that blood contamination was producing our results, although our results in mice indicated an extravascular location.[7] We found a few intravascular HSPCs, confirming previous studies, but the vast majority were extravascular and predominately in vascular-rich zones of the lung alveoli. This anatomic location in the lung is similar to the location of HSPCs in the BM, which are closely positioned next to the vascular sinusoids.[37,38] In the lung, this positioning could be important for seeding of the lung with circulating HSCs and potentially for exiting the lung during hematopoietic stress. In this niche, it was notable that lung fibroblasts were in close proximity. The lung mesenchyme is well known to be a critical niche supporting epithelial cell development and repair and similar mechanisms could be operable influencing lung HSPCs.[39,40] Also, we identified a developmental trajectory between lung HSPCs and lung stromal cells. Subpopulations of lung fibroblasts are known to be $CD34^+$ and previous lineage-tracing experiments in pulmonary fibrosis have shown a hematopoietic contribution to fibroblasts.[41,42] Future studies are needed in this area to understand how lung HSPCs could be involved in fibrotic lung diseases.

We have not addressed the ontogeny of lung HSPCs—something not possible given the restraints of our human tissue study. There is irrefutable evidence that HSCs commonly enter the circulation and microcirculatory beds, and given the functional and molecular similarities of lung HSPCs to other extramedullary HSPCs, this is perhaps the source of the tissue resident HSPCs in the lung.[35,43] There is precedence, however, for tissue residency to be endowed during development, such as with yolk-sac derived macrophages.[44] Future studies will be needed to answer this question in mice, including the possibility that hemogenic endothelium in the fetal lung could be the source.[45]

Our findings reframe our understanding of the HSPC pool and its molecular diversity and should enable future studies that could potentially lead to therapeutic advances, such as for life-saving HSC transplantation for BM malignancies and failure. In the modern era, transplantation is mainly

accomplished using mobilized HSCs obtained from the peripheral blood. We propose that these mobilized cells are sourced from diverse tissues, including the lung, and that the composition of this pool may be functionally heterogeneous, which could have important implications for treatment responses and complications. In this regard, our findings may also help to understand the mechanisms of leukemogenesis with the possibility that lung HSPCs are direct targets of environmental carcinogens.[46] Further, our findings add to our expanding understanding of rare cell types in the lung and their potential functions.[47]

Declarations

Acknowledgements

We thank Donor Network West and Michael Matthay (UCSF) for providing human lung tissue from deceased organ donors. This work was supported by an IARS Mentored Research Award to C.C., the Deutsche Forschungsgemeinschaft (DFG) Research Fellowships to C.C. (CO 2096/1-1) and N.M. (ME 5209/1-1), Bakar UCSF ImmunoX support to A.J.C, a Wellcome-Royal Society Sir Henry Dale Fellowship (107630/Z/15/Z) and funding in part by the Wellcome Trust [203151/Z/16/Z, 203151/A/16/Z] and the UKRI Medical Research Council [MC_PC_17230] to E.L., and NIH R35HL161241 to M.R.L. Sequencing was performed at the UCSF CAT, supported by UCSF PBBR, RRP IMIA, and NIH 1S10OD028511-01 grants. For the purpose of open access, E.L. has applied a CC BY public copyright licence to any Author Accepted Manuscript version arising from this submission.

Author contributions

C.C. designed and conducted experiments, analyzed the data, and wrote the manuscript. M.M. and designed and conducted experiments. J.T, B.S., U.V. and A.J.C. assisted in designing and conducting experiments, and helped analyzing the data. H.W. and M.N. helped analyzing the data. S.J.C., L.Q., J.J.T. and M.D.G. assisted in conducting experiments. E.P., E.L. and N.M. assisted in designing experiments, provided technical expertise with hematopoietic progenitor analyses, and provided editorial support on the manuscript. M.R.L. designed the experiments, supervised the study and wrote the manuscript.

The authors declare no competing financial interests.

References

1. Weissman, I.L., and Shizuru, J.A. (2008). The origins of the identification and isolation of hematopoietic stem cells, and their capability to induce donor-specific transplantation tolerance and treat autoimmune diseases. Blood *112*, 3543-3553. 10.1182/blood-2008-08-078220.

2. Abkowitz, J.L., Catlin, S.N., McCallie, M.T., and Guttorp, P. (2002). Evidence that the number of hematopoietic stem cells per animal is conserved in mammals. Blood *100*, 2665-2667. 10.1182/blood-2002-03-0822.

3. Nombela-Arrieta, C., and Manz, M.G. (2017). Quantification and three-dimensional microanatomical organization of the bone marrow. Blood Adv *1*, 407-416. 10.1182/bloodadvances.2016003194.

4. Wilkinson, A.C., Igarashi, K.J., and Nakauchi, H. (2020). Haematopoietic stem cell self-renewal in vivo and ex vivo. Nat Rev Genet *21*, 541-554. 10.1038/s41576-020-0241-0.

5. Verovskaya, E.V., Dellorusso, P.V., and Passegue, E. (2019). Losing Sense of Self and Surroundings: Hematopoietic Stem Cell Aging and Leukemic Transformation. Trends Mol Med *25*, 494-515. 10.1016/j.molmed.2019.04.006.

6. Jaiswal, S., and Ebert, B.L. (2019). Clonal hematopoiesis in human aging and disease. Science *366*. 10.1126/science.aan4673.

7. Lefrançais, E., Ortiz-Muñoz, G., Caudrillier, A., Mallavia, B., Liu, F., Sayah, D.M., Thornton, E.E., Headley, M.B., David, T., Coughlin, S.R., et al. (2017). The lung is a site of platelet biogenesis and a reservoir for haematopoietic progenitors. Nature *544*, 105-109. 10.1038/nature21706.

8. Notta, F., Doulatov, S., Laurenti, E., Poeppl, A., Jurisica, I., and Dick, J.E. (2011). Isolation of single human hematopoietic stem cells capable of long-term multilineage engraftment. Science *333*, 218-221. 10.1126/science.1201219.

9. Notta, F., Zandi, S., Takayama, N., Dobson, S., Gan, O.I., Wilson, G., Kaufmann, K.B., McLeod, J., Laurenti, E., Dunant, C.F., et al. (2016). Distinct routes of lineage development reshape the human blood hierarchy across ontogeny. Science *351*, aab2116. 10.1126/science.aab2116.

10. Sanada, C., Xavier-Ferrucio, J., Lu, Y.C., Min, E., Zhang, P.X., Zou, S., Kang, E., Zhang, M., Zerafati, G., Gallagher, P.G., and Krause, D.S. (2016). Adult human megakaryocyte-erythroid progenitors are in the CD34+CD38mid fraction. Blood *128*, 923-933. 10.1182/blood-2016-01-693705.

11. Green, J., Endale, M., Auer, H., and Perl, A.K. (2016). Diversity of Interstitial Lung Fibroblasts Is Regulated by Platelet-Derived Growth Factor Receptor α Kinase Activity. Am J Respir Cell Mol Biol *54*, 532-545. 10.1165/rcmb.2015-0095OC.

12. Belluschi, S., Calderbank, E.F., Ciaurro, V., Pijuan-Sala, B., Santoro, A., Mende, N., Diamanti, E., Sham, K.Y.C., Wang, X., Lau, W.W.Y., et al. (2018). Myelo-lymphoid lineage restriction occurs in the human haematopoietic stem cell compartment before lymphoid-primed multipotent progenitors. Nat Commun *9*, 4100. 10.1038/s41467-018-06442-4.

13. Nicolini, F.E., Cashman, J.D., Hogge, D.E., Humphries, R.K., and Eaves, C.J. (2004). NOD/SCID mice engineered to express human IL-3, GM-CSF and Steel factor constitutively mobilize engrafted human progenitors and compromise human stem cell regeneration. Leukemia *18*, 341-347. 10.1038/sj.leu.2403222.

14. Park, C.Y., Majeti, R., and Weissman, I.L. (2008). In vivo evaluation of human hematopoiesis through xenotransplantation of purified hematopoietic stem cells from umbilical cord blood. Nat Protoc *3*, 1932-1940. 10.1038/nprot.2008.194.

15. McKenzie, J.L., Takenaka, K., Gan, O.I., Doedens, M., and Dick, J.E. (2007). Low rhodamine 123 retention identifies long-term human hematopoietic stem cells within the Lin-CD34+CD38- population. Blood *109*, 543-545. 10.1182/blood-2006-06-030270.

16. Goyama, S., Wunderlich, M., and Mulloy, J.C. (2015). Xenograft models for normal and malignant stem cells. Blood *125*, 2630-2640. 10.1182/blood-2014-11-570218.

17. Korsunsky, I., Millard, N., Fan, J., Slowikowski, K., Zhang, F., Wei, K., Baglaenko, Y., Brenner, M., Loh, P.R., and Raychaudhuri, S. (2019). Fast, sensitive and accurate integration of single-cell data with Harmony. Nat Methods *16*, 1289-1296. 10.1038/s41592-019-0619-0.

18. Hay, S.B., Ferchen, K., Chetal, K., Grimes, H.L., and Salomonis, N. (2018). The Human Cell Atlas bone marrow single-cell interactive web portal. Exp Hematol *68*, 51-61. 10.1016/j.exphem.2018.09.004.

19. Travaglini, K.J., Nabhan, A.N., Penland, L., Sinha, R., Gillich, A., Sit, R.V., Chang, S., Conley, S.D., Mori, Y., Seita, J., et al. (2020). A molecular cell atlas of the human lung from single-cell RNA sequencing. Nature *587*, 619-625. 10.1038/s41586-020-2922-4.

20. Cao, J., Spielmann, M., Qiu, X., Huang, X., Ibrahim, D.M., Hill, A.J., Zhang, F., Mundlos, S., Christiansen, L., Steemers, F.J., et al. (2019). The single-cell transcriptional landscape of mammalian organogenesis. Nature *566*, 496-502. 10.1038/s41586-019-0969-x.

21. Sato, A., Kamio, N., Yokota, A., Hayashi, Y., Tamura, A., Miura, Y., Maekawa, T., and Hirai, H. (2020). C/EBPβ isoforms sequentially regulate regenerating mouse hematopoietic stem/progenitor cells. Blood Adv *4*, 3343-3356. 10.1182/bloodadvances.2018022913.

22. Mohanty, J.G., Nagababu, E., Friedman, J.S., and Rifkind, J.M. (2013). SOD2 deficiency in hematopoietic cells in mice results in reduced red blood cell deformability and increased heme degradation. Exp Hematol *41*, 316-321. 10.1016/j.exphem.2012.10.017.

23. Barbosa, C.M., Bincoletto, C., Barros, C.C., Ferreira, A.T., and Paredes-Gamero, E.J. (2014). PLCγ2 and PKC are important to myeloid lineage commitment triggered by M-SCF and G-CSF. J Cell Biochem *115*, 42-51. 10.1002/jcb.24653.

24. Kruta, M., Sunshine, M.J., Chua, B.A., Fu, Y., Chawla, A., Dillingham, C.H., Hidalgo San Jose, L., De Jong, B., Zhou, F.J., and Signer, R.A.J. (2021). Hsf1 promotes hematopoietic stem cell fitness and proteostasis in response to ex vivo culture stress and aging. Cell Stem Cell *28*, 1950-1965.e1956. 10.1016/j.stem.2021.07.009.

25. Pariser, D.N., Hilt, Z.T., Ture, S.K., Blick-Nitko, S.K., Looney, M.R., Cleary, S.J., Roman-Pagan, E., Saunders, J., 2nd, Georas, S.N., Veazey, J., et al. (2021). Lung megakaryocytes are immune modulatory cells. J Clin Invest *131*. 10.1172/JCI137377.

26. Sikkema, L., Ramírez-Suástegui, C., Strobl, D.C., Gillett, T.E., Zappia, L., Madissoon, E., Markov, N.S., Zaragosi, L.E., Ji, Y., Ansari, M., et al. (2023). An integrated cell atlas of the lung in health and disease. Nat Med *29*, 1563-1577. 10.1038/s41591-023-02327-2.

27. https://azimuth.hubmapconsortium.org/references/#Human%20-%20Lung%20v2%20%28HLCA%29.

28. Palla, G., Spitzer, H., Klein, M., Fischer, D., Schaar, A.C., Kuemmerle, L.B., Rybakov, S., Ibarra, I.L., Holmberg, O., Virshup, I., et al. (2022). Squidpy: a scalable framework for spatial omics analysis. Nat Methods *19*, 171-178. 10.1038/s41592-021-01358-2.

29. Ghersi, J.J., Baldissera, G., Hintzen, J., Luff, S.A., Cheng, S., Xia, I.F., Sturgeon, C.M., and Nicoli, S. (2023). Haematopoietic stem and progenitor cell heterogeneity is inherited from the embryonic endothelium. Nat Cell Biol *25*, 1135-1145. 10.1038/s41556-023-01187-9.

30. Zhang, Y., and Liu, F. (2023). The evolving views of hematopoiesis: from embryo to adulthood and from in vivo to in vitro. J Genet Genomics. 10.1016/j.jgg.2023.09.005.

31. Mende, N., Bastos, H.P., Santoro, A., Mahbubani, K.T., Ciaurro, V., Calderbank, E.F., Quiroga Londono, M., Sham, K., Mantica, G., Morishima, T., et al. (2022). Unique molecular and functional features of extramedullary hematopoietic stem and progenitor cell reservoirs in humans. Blood *139*, 3387-3401. 10.1182/blood.2021013450.

32. Imataki, O., Ohnishi, H., Kushida, Y., Kitanaka, A., and Kubota, Y. (2008). Pulmonary extramedullary haematopoiesis after allogeneic stem-cell transplantation. Transplantation *85*, 1510-1512. 10.1097/TP.0b013e318170592f.

33. Spencer, J.A., Ferraro, F., Roussakis, E., Klein, A., Wu, J., Runnels, J.M., Zaher, W., Mortensen, L.J., Alt, C., Turcotte, R., et al. (2014). Direct measurement of local oxygen concentration in the bone marrow of live animals. Nature *508*, 269-273. 10.1038/nature13034.

34. Li, D., Xue, W., Li, M., Dong, M., Wang, J., Wang, X., Li, X., Chen, K., Zhang, W., Wu, S., et al. (2018). VCAM-1(+) macrophages guide the homing of HSPCs to a vascular niche. Nature *564*, 119-124. 10.1038/s41586-018-0709-7.

35. Massberg, S., Schaerli, P., Knezevic-Maramica, I., Kollnberger, M., Tubo, N., Moseman, E.A., Huff, I.V., Junt, T., Wagers, A.J., Mazo, I.B., and von Andrian, U.H. (2007). Immunosurveillance by hematopoietic progenitor cells trafficking through blood, lymph, and peripheral tissues. Cell *131*, 994-1008. 10.1016/j.cell.2007.09.047.

36. Wright, D.E., Wagers, A.J., Gulati, A.P., Johnson, F.L., and Weissman, I.L. (2001). Physiological migration of hematopoietic stem and progenitor cells. Science *294*, 1933-1936. 10.1126/science.1064081.

37. Acar, M., Kocherlakota, K.S., Murphy, M.M., Peyer, J.G., Oguro, H., Inra, C.N., Jaiyeola, C., Zhao, Z., Luby-Phelps, K., and Morrison, S.J. (2015). Deep imaging of bone marrow shows non-dividing stem cells are mainly perisinusoidal. Nature *526*, 126-130. 10.1038/nature15250.

38. Kiel, M.J., Yilmaz, O.H., Iwashita, T., Yilmaz, O.H., Terhorst, C., and Morrison, S.J. (2005). SLAM family receptors distinguish hematopoietic stem and progenitor cells and reveal endothelial niches for stem cells. Cell *121*, 1109-1121. 10.1016/j.cell.2005.05.026.

39. Cao, Z., Lis, R., Ginsberg, M., Chavez, D., Shido, K., Rabbany, S.Y., Fong, G.H., Sakmar, T.P., Rafii, S., and Ding, B.S. (2016). Targeting of the pulmonary capillary vascular niche promotes lung alveolar repair and ameliorates fibrosis. Nat Med *22*, 154-162. 10.1038/nm.4035.

40. Mammoto, A., and Mammoto, T. (2019). Vascular Niche in Lung Alveolar Development, Homeostasis, and Regeneration. Front Bioeng Biotechnol *7*, 318. 10.3389/fbioe.2019.00318.

41. Phan, S.H. (2012). Genesis of the myofibroblast in lung injury and fibrosis. Proc Am Thorac Soc *9*, 148-152. 10.1513/pats.201201-011AW.

42. Reilkoff, R.A., Bucala, R., and Herzog, E.L. (2011). Fibrocytes: emerging effector cells in chronic inflammation. Nat Rev Immunol *11*, 427-435. 10.1038/nri2990.

43. Ceradini, D.J., Kulkarni, A.R., Callaghan, M.J., Tepper, O.M., Bastidas, N., Kleinman, M.E., Capla, J.M., Galiano, R.D., Levine, J.P., and Gurtner, G.C. (2004). Progenitor cell trafficking is regulated by hypoxic gradients through HIF-1 induction of SDF-1. Nat Med *10*, 858-864. 10.1038/nm1075.

44. Gomez Perdiguero, E., Klapproth, K., Schulz, C., Busch, K., Azzoni, E., Crozet, L., Garner, H., Trouillet, C., de Bruijn, M.F., Geissmann, F., and Rodewald, H.R. (2015). Tissue-resident macrophages originate from yolk-sac-derived erythro-myeloid progenitors. Nature *518*, 547-551. 10.1038/nature13989.

45. Yeung, A.K., Villacorta-Martin, C., Lindstrom-Vautrin, J., Belkina, A.C., Vanuytsel, K., Dowrey, T.W., Ysasi, A.B., Bawa, P., Wang, F., Vrbanac, V., et al. (2023). De novo hematopoiesis from the fetal lung. Blood Adv *7*, 6898-6912. 10.1182/bloodadvances.2022008347.

46. Zhao, Y., Magaña, L.C., Cui, H., Huang, J., McHale, C.M., Yang, X., Looney, M.R., Li, R., and Zhang, L. (2021). Formaldehyde-induced hematopoietic stem and progenitor cell toxicity in mouse lung and nose.

Arch Toxicol *95*, 693-701. 10.1007/s00204-020-02932-x.

47. Montoro, D.T., Haber, A.L., Biton, M., Vinarsky, V., Lin, B., Birket, S.E., Yuan, F., Chen, S., Leung, H.M., Villoria, J., et al. (2018). A revised airway epithelial hierarchy includes CFTR-expressing ionocytes. Nature *560*, 319-324. 10.1038/s41586-018-0393-7.

Figures

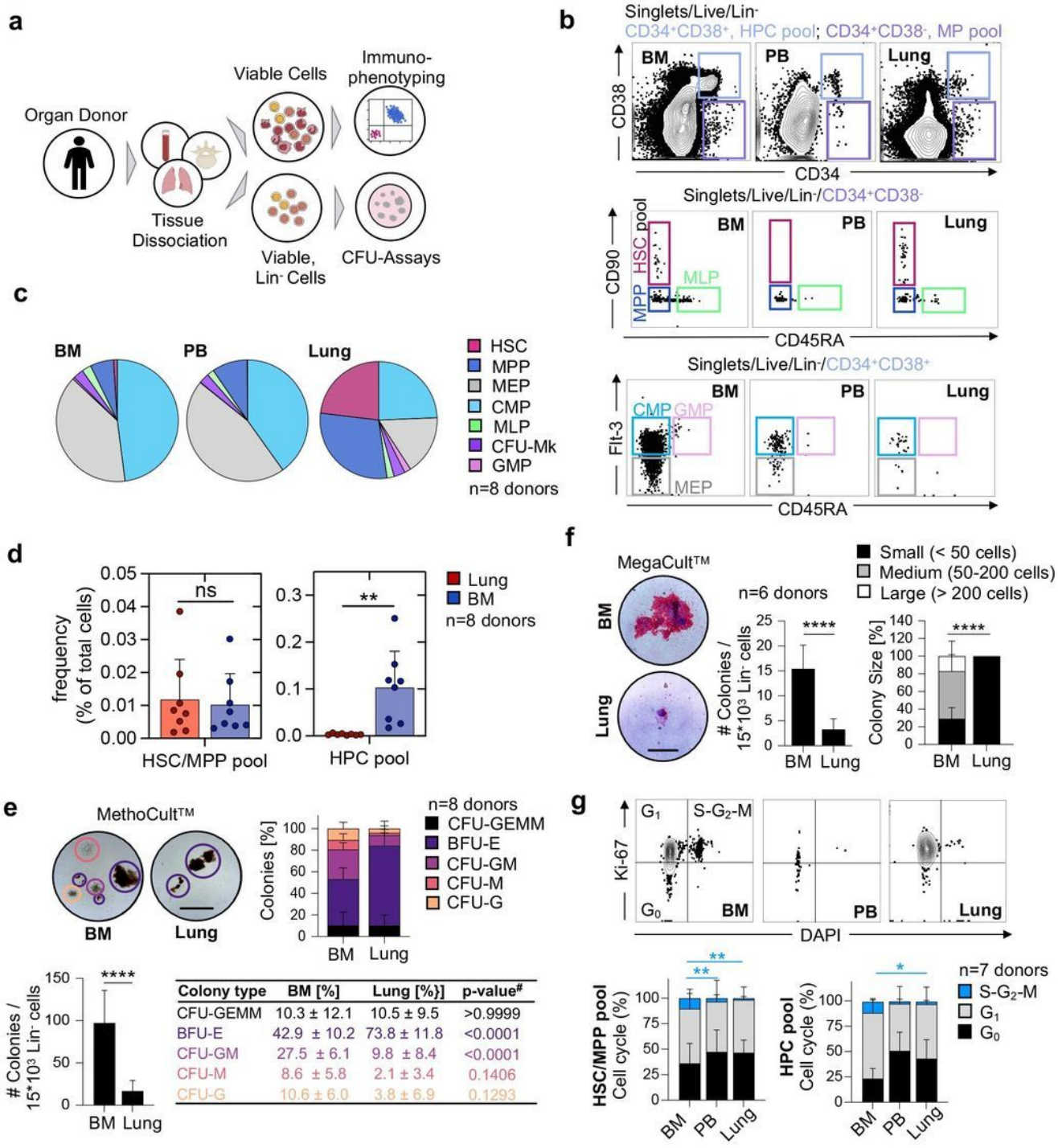

Figure 1

The human lung contains phenotypic hematopoietic progenitors with in vitro proliferation and differentiation capacity. (A) Pipeline for flow-cytometric immunophenotyping and evaluation of in vitro colony-forming capacity of hematopoietic progenitor cells from BM, lung and PB of organ donors. (B) Normalized flow cytometry plots of BM, PB in the Live/Lin- gate from a representative donor showing stem cell subsets within the multipotent (MP [CD34+CD38-], light purple) and the hematopoietic progenitor cell (HPC [CD34+CD38+], light blue) pool. HSC, hematopoietic stem cell; MPP, multipotent progenitor; MLP, multilymphoid progenitor; CMP, common myeloid progenitor; MEP, megakaryocyte-erythroid progenitor; GMP, granulocyte-macrophage progenitor; CFU-Mk, colony-forming-unit megakaryocyte. (C) Composition of hematopoietic progenitor subsets in the BM, PB and lung (n=8). (D) Frequency of cells in the HSC/MPP and HPC pool as a percentage of total nucleated cells in the lung or BM, respectively. Individual values are shown, bars represent mean ± SD. Student's t-test, **p<0.01; ns, not significant. (E) Culture initiating capacity of lung and BM progenitors in MethoCultTM (n=8): Representative colonies (scale bar, 500µm), colony composition and colony quantity for progenitors derived from the BM and lung. Student's t-test, ****p<0.0001, #ANOVA followed by Sidak's multiple comparison test. CFU, colony-forming unit; BFU-E (purple), burst-forming unit-erythroid; G (orange), granulocyte; M (red), macrophage; GM (pink), granulocyte macrophage; GEMM (black), granulocyte, erythroid, macrophage, megakaryocyte. (F) Culture initiating capacity of lung and BM progenitors in MegaCultTM (n=6): Representative colonies (scale bar, 100µm), colony quantity and colony size for progenitors from the BM and lung. Bar graph represents mean number of colonies ± SD, Student's t-test, ****p<0.0001. Stacked bars represent mean proportion ± SD, Kruskal-Wallis test, ****p<0.0001. (G) Proportions of cycling (S-G2-M phase (blue), Ki-67+DAPI+), preparing/growing (G1 (grey), Ki-67+DAPI-) and resting cells (G0 (black), Ki-67-DAPI-) in the HSC/MPP and HPC pool from BM, PB and lung (n=7). Stacked bars represent mean proportion ± SD, ANOVA followed by Sidak's multiple comparison test, **p<0.01, *p<0.05. For comparisons not indicated, no statistically significant differences were observed.

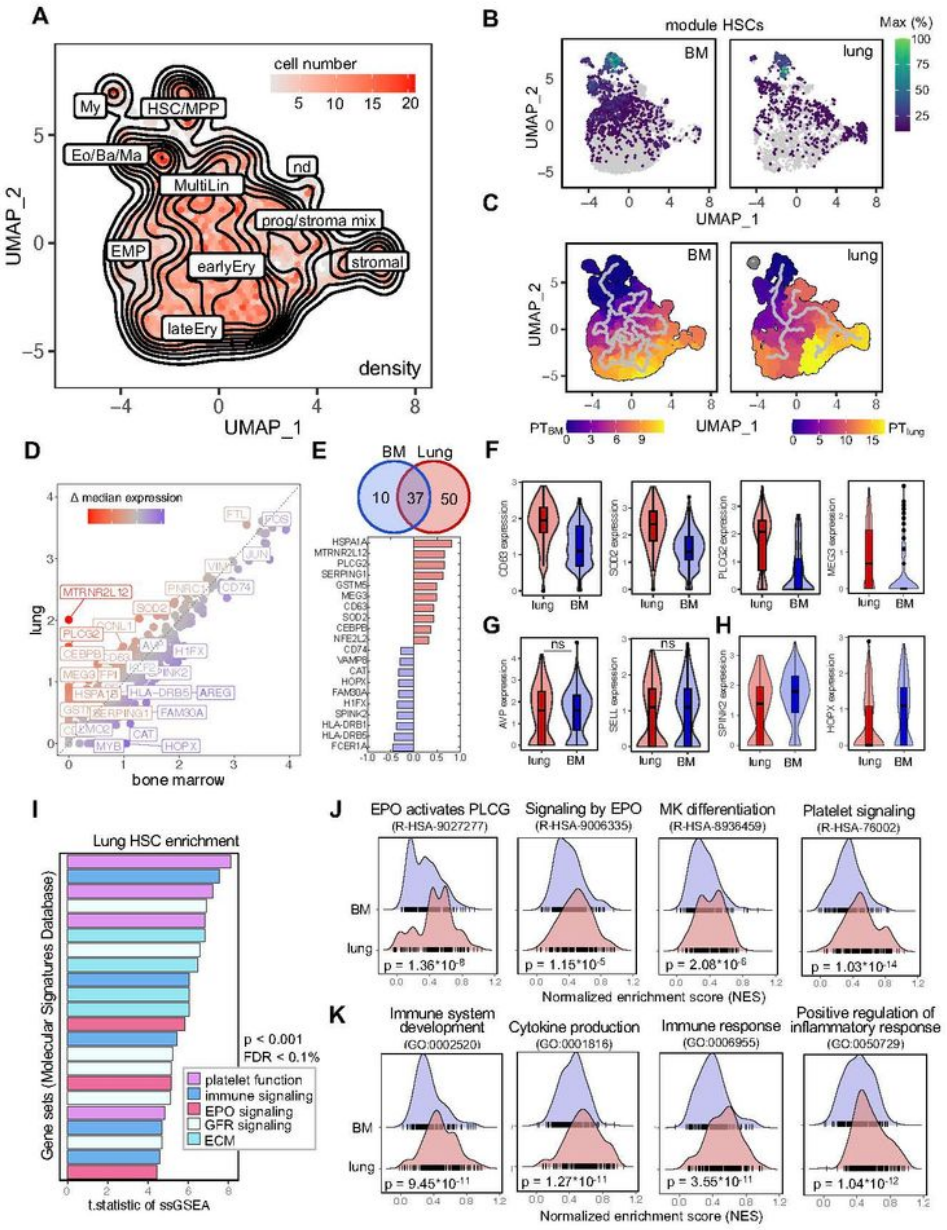

Figure 3

Figure 3

Comparative transcriptomic analysis of lung and BM HSCs reveals shared and unique gene expression profiles. (A) Annotated, batch-corrected UMAP projection with cell density representation of merged BM and lung Lin-CD34+ progenitor subsets from 8 human donors. HSC/MPP, hematopoietic stem cell/multipotent progenitor; My, myeloid cell; Eo/Ba/Ma, eosinophil/basophil/mast cell progenitor; MultiLin, multi-lineage; EMP, erythroid megakaryocytic progenitor; earlyEry, early erythroid progenitor;

lateEry, late erythroid progenitor; prog/stroma mix, progenitor stroma cell mix; nd, not determined. (B) Grouping of gene expression patterns into modules using Monocle3. Aggregate expression values of genes in the module highly specific for HSCs (Figure S6) are shown individually for the BM and lung. (C) Pseudotime calculation for each cell within the BM and lung using Monocle3 to infer progression through different cellular differentiation to provide insights into the developmental trajectory. (D) Scatter plot of median gene expression of cells in the HSC/MPP cluster from the lung (red) and BM (blue) to visualize consistent (grey) and differentially (highlighted) expressed genes. (E) Venn diagram and top 10 differentially expressed genes. The number in each circle represents the amount of differentially expressed genes between lung (red) and BM (blue), the overlapping number indicates mutual differentially expressed genes based on the Wilcoxon ran-sum test in Seurat's 'FindMarkers' function. (F) Box and violin plots showing the distribution of selected genes upregulated in pulmonary hematopoietic progenitor cells. Wilcoxon adjusted p-value <0.001. (G) Selection of marker genes shared between lung and BM as box and violin plots, respectively. ns, not significant. (H) Box and violin plots showing the distribution of markers genes upregulated in BM HSCs, Wilcoxon adjusted p-value <0.001. (I) T.statistic of ssGSEA scores for selected gene sets (Hallmark, Reactome, Biocarta, KEGG) enriched in pulmonary HSCs categorized by recurring functions. EPO, erythropoietin; ECM, extracellular matrix, FDR, false discovery rate; GFR, growth factor receptor; ssGSEA, single-sample Gene Set Enrichment Analysis. (J) Enrichment ridge plots comparing the distribution of enrichment scores in HSCs from lung (red) and BM (blue) of selected Reactome pathways. Rug plots indicate the scores of individual cells along the ridge plot. P-values are given in the figure, FDR R-HSA-9027277 = 2.38*10-4; FDR R-HSA-9006335 = 0.09; FDR R-HSA-8936459 = 0.03; R-HSA-76002 = 2.03*10-10. (K) Enrichment ridge plots showing the distribution of enrichment scores in lung (red) and BM (blue) with individual cell placement on the rug plot to compare selected GOBP (Gene Ontology Biological Process) gene set enrichments. P-values are given in the figure, FDR GO:0002520 = 1.77*10-6; FDR GO:0001816 = 2.42*10-7; FDR GO:0006955 = 6.70*10-7; GO:0050729 = 2.02*10-8.

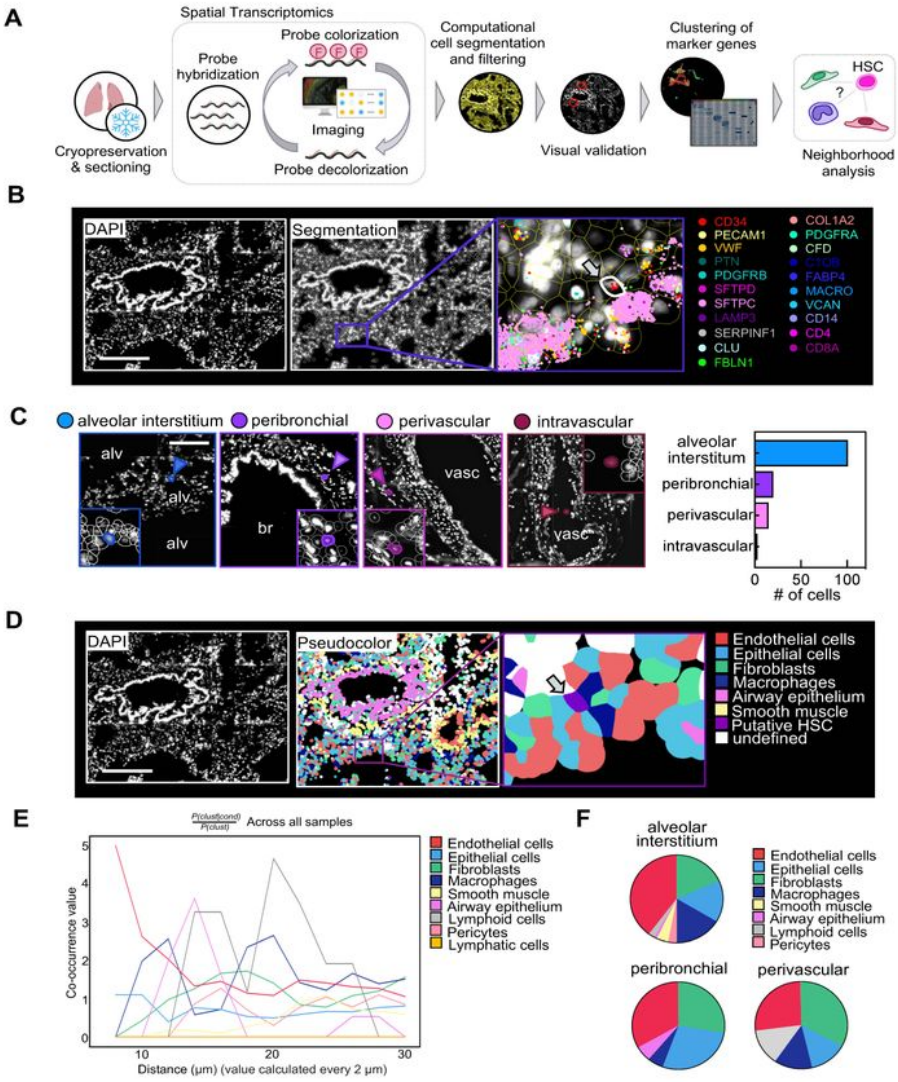

Figure 4

Figure 4

Spatial mapping of phenotypic CD34+ HSPCs in the lung. (A) Spatial transcriptomics analysis workflow. smFISH was performed to visualize gene expression in human lung tissue. Transcripts were assigned to individual cells after cell segmentation and putative HSPCs were computationally identified based on their gene signature and visually validated. Lung stromal and immune cells were annotated based on marker gene clusters (Figure S8). Subsequently, co-occurence analysis was performed. (B) Representative

image of a putative HSPC in its pulmonary niche. Upper panel (left to right): DAPI staining, QuPath segmentation, zoom on putative HSC (arrow). Selected transcripts are shown. Scale bar, 250 µm (C) Anatomic location of candidate cells in the lung. Representative images of phenotypic HSPCs in four major locations (alveolar interstitium, peribronchial, perivascular or intravascular) and proportion of cells in each location. Alv, alveolar space; br, bronchus; vasc, vasculature. Scale bar, 150µm. (D) Pseudo-coloring of cell types in the lung tissue based on marker clustering (Figure S8). Zoom on putative HSPC in niche. Scale bar, 250 µm. (E) Squidpy co-occurrence score computed every 2 µm between putative HSPCs and the rest of the clusters across lung tissue sections from 4 organ donors. High score values indicate greater co-occurrence probability; endothelial cells (red) and macrophages (dark blue) co-occur with the HSPCs at short distances. (F) Pie graphs showing the proportion of neighboring cells within a radius of 20 µm from the putative HSPCs in the major anatomic locations.

Supplementary Files

This is a list of supplementary files associated with this preprint. Click to download.

- SupplementalTables.pdf
- KeyResourcesTable.docx
- MethodsSupplementaryFiguresFINAL.pdf
- SupplementalFigurescomp.pdf